Original Article

PMP
Progress in Medical Physics 32(4), December 2021
https://doi.org/10.14316/pmp.2021.32.4.159
eISSN 2508-4453

Assessing Commercial CLEANBOLUS Based on Silicone for Clinical Use

Jaeman Son[1,2], Seongmoon Jung[1,2], Jong Min Park[1,2,3,4], Chang Heon Choi[1,2,3], Jung-in Kim[1,2,3]

[1]Department of Radiation Oncology, Seoul National University Hospital, [2]Institute of Radiation Medicine, Seoul National University Medical Research Center, [3]Biomedical Research Institute, Seoul National University Hospital, [4]Department of Radiation Oncology, Seoul National University College of Medicine, Seoul, Korea

Received 2 December 2021
Revised 16 December 2021
Accepted 20 December 2021

Corresponding author
Jung-in Kim
(madangin@gmail.com)
Tel: 82-2-2072-3573
Fax: 82-2-3410-2619

Purpose: We investigated the properties of CLEANBOLUS based on silicone with suitable characteristics for clinical use.
Methods: We evaluated the characteristics of CLEANBOLUS and compared the results with the commercial product (Super-Flex bolus). Also, we conducted physical evaluations, including shore hardness, element composition, and elongation break. Transparency was investigated through the measured absorbance within the visible region (400–700 nm). Also, dosimetric characteristics were investigated with surface dose and beam quality. Finally, the volume of unwanted air gap was investigated based on computed tomography images for breast, chin, and nose using Super-Flex bolus and CELANBOLUS.
Results: CLEANBOLUS showed excellent physical properties for a low shore hardness (000–35) and elongation break (>1,000%). Additionally, it was shown that CLEANBOLUS is more transparent than Super-Flex bolus. Dosimetric results obtained through measurement and calculation have an electron density similar to water in CLEANBOLUS. Finally, CLEANBOLUS showed that the volume of unwanted air gap between the phantom and each bolus is smaller than Super-Flex bolus for breast, chin, and nose.
Conclusions: The physical properties of CLEANBOLUS, including excellent adhesive strength and lower shore hardness, reduce unwanted air gaps and ensure accurate dose distribution. Therefore, it would be an alternative to other boluses, thus improving clinical use efficiency.

Keywords: Bolus, Transparency, Surface dose, Air gap

Introduction

High-energy megavoltage (MV) photon beams are most widely used in external radiation therapy for tumor treatment because they can penetrate deeply into a site [1-3]. These high-energy MV photon beams can deliver more doses to a point more than a certain depth than the surface. The region from the surface to a certain depth is called the buildup region, a part that should always be considered when treating patients using high-energy MV photon beams [4-9]. In the buildup region, the dose delivered to the patient's skin is relatively small due to the skin-sparing effect in high-energy MV photon therapy. For example, even if a high dose is delivered to a deep tumor, the dose delivered to the skin surface is low. However, these advantages can be disadvantageous. To deliver prescription doses to tumors close to the surface, more doses are delivered even if there is no tumor in the maximum dose depth [10-12]. To overcome these drawbacks, a bolus is used to treat photon beams, allowing as much dose to be delivered to

the tumor [11,13,14]. Properties that adhere closely to the skin are essential for use as a bolus. If it does not adhere to the skin, an unwanted air gap occurs between the skin and the bolus, affecting dose delivery dosimetrically. Butson et al. [15] reported that for a 6-MV photon beam, 4- and 10-mm air gaps reduce dosage by 4% and 10%, respectively. Also, bolus characteristics are needed to help calibrate with a high-energy MV photon beam in an energy range greater than 1 MeV. This assures accurate measurement and administration of the prescribed radiation dose. Additionally, it is transparent to allow visual beam location. Materials do not flow, creep, and sag out of shape and can be cut with scissors to fit the patient and layered as required to build up thickness. The CLEANBOLUS (Paprica Lab, Seoul, Korea) was recently released with various bolus features. It is flexible to adhere to the skin and transparent, with properties suitable for clinical use. This study evaluated the physical and dosimetric characteristics for CLEANBOLUS and compared it with a commercial Super-Flex bolus (Radiation Products Design Inc, Albertville, MN, USA).

Materials and Methods

1. Physical evaluations

CLEANBOLUS is manufactured from liquid silicone compounds, evaluated as a nonirritant according to OECD 439 (in vitro skin irritation) protocol. The mass density, electron density, elongation at break, and shore hardness were investigated to evaluate the physical properties. For each CLEANBOLUS material, the effective atomic number (Z_{eff}) was obtained from the elemental analysis results using X-ray fluorescence (XRF). Elements were identified using their characteristic XRF emissions (voltage: 60 kV, current: 170 mA), and XRF intensity is proportional to the concentrations of elements in the samples. Besides, we used boluses of 5- and 10-mm thickness to measure the transparency of each bolus. The transparency of each material was investigated through the measured absorbance within the visible region (400–700 nm) using the Eppendorf BioSpectrometer (Eppendorf, Hamburg, Germany).

2. Dosimetric evaluation

To evaluate dosimetric properties, we measured the CT number for each bolus. The surface dose and beam quality were obtained from a treatment planning system (TPS) (Eclipse; Varian Medical Systems, Palo Alto, CA, USA) to evaluate the dosimetric effect of each bolus. Also, the thickness of each bolus was set to 1 cm and was compared dosimetrically with the thickness of water set to 1 cm. A high-energy MV photon beam (6, 10, and 15 MV) was used with a 10×10 cm^2 open field and a source surface distance (SSD) of 100 cm from the surface of the water phantom in the TPS. Furthermore, dose distributions for 100 monitor units (MU) with a grid size of 1 mm were calculated. Each beam was calibrated to deliver 1.0 cGy/MU at a maximum dose depth according to the American Association of Physicists in Medicine task group-51 protocol. Also, dosimetric evaluation was verified through measurement at SSD=100 cm, field size=10×10 cm^2, and 2 cm depth using a solid water phantom. Next, a 0.125 cc chamber (PTW 31010; PTW, Freiburg, Germany) was used, and a thickness of 2 cm was set by mixing each bolus with the solid phantom. Next, the bolus was positioned on the surface for each part using Rando phantom to investigate the volume of the unwanted air gap generated between the surface and bolus. Also, we cut the CLEANBOLUS (30×30 cm^2) with scissors to fit and attach the part. Then, computed tomography (CT; Big Bore RT; Philips, Amsterdam, Netherlands) scans were performed to calculate the volume of unwanted air gap between each bolus and phantom using TPS contouring function. After that, Super-Flex bolus and CLEANBOLUS were placed on the surface of the Rando phantom, respectively.

Results

1. Physical properties

Table 1 summarizes the physical properties of CLEANBOLUS. CLEANBOLUS shows a relatively low shore hardness and elongation at break for Super-Flex bolus. The shore hardness of CLEANBOLUS, indicating the material's rigidity, is an important property. Super-Flex bolus' shore hardness is unknown numerically, but CLEANBOLUS is

Table 1. Physical characteristics of Super-Flex bolus and CLEANBOLUS

Physical properties	Super-Flex bolus	CLEANBOLUS
Mass density (g cc^{-1})	1.03	0.98
Relative electron density to water	1.02	1.04
Elongation at break (%)	1,030	>1,000
Shore hardness	Unknown	000-35 (Extra soft)

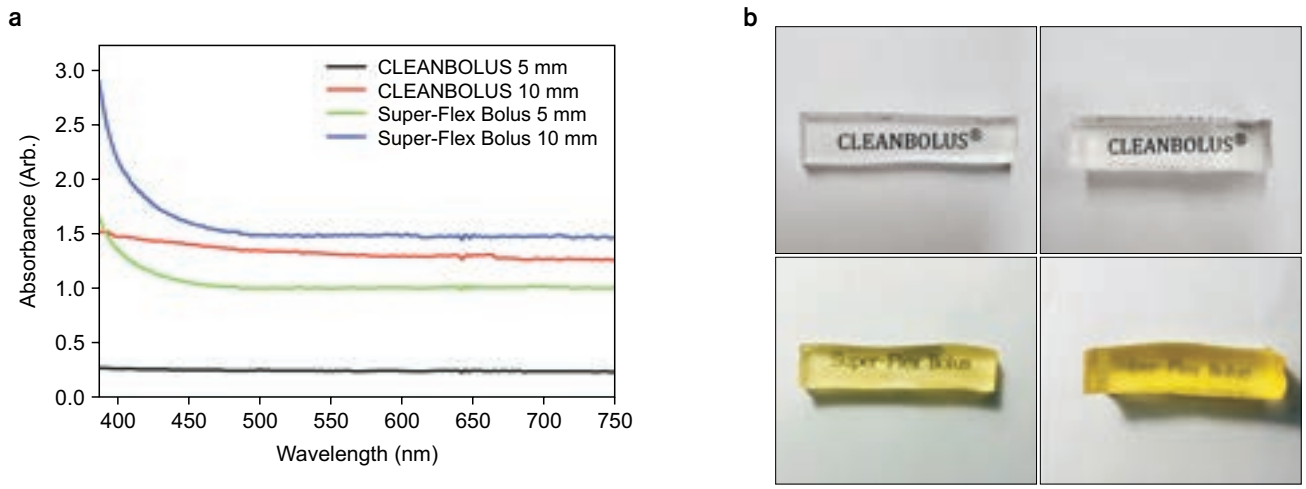

Fig. 1. Absorbance from 400 nm to 750 nm (a) and pictures showing the transparency of the for Super-Flex bolus and CLEANBOLUS of 5 mm and 10 mm thicknesses under normal room lighting conditions (b).

softer than Super-Flex bolus due to direct use. This result means that CLEANBOLUS can be attached to irregular skin surfaces. For example, Fig. 1 shows the results of transparency for each bolus. In the graph, the y-axis is absorbance, and the lower it is, the more transparent it becomes. For example, the area in the visible light region (400–700 nm) is 74.2 nm·A for CLEANBOLUS and 312.6 nm·A for Super-Flex bolus at 5 mm thickness, indicating that CLEANBOLUS is more transparent.

Similarly, at a thickness of 10 mm, the CLEANBOLUS is 404.2, and the Super-Flex bolus is 466.7, showing the same results. Table 2 indicates the elemental compositions of CLEANBOLUS obtained through XRF measurements. For example, Si accounted for the largest percentage, flowed by C, H, O, Si, Na, Cl, K, Al, S, Ca, Fe, and Zn. Based on elemental compositions, Zeff was calculated at about 23.87. Additionally, the ratio of the atomic number and mass of each element (Z/A) was about 0.54.

Table 2. Component of CLEANBOLUS

Formula	Z	Concentration
Si	14	57.19%
C	6	32.20%
H	1	8.26%
Na	11	1.34%
Cl	17	0.36%
O	8	0.29%
K	19	0.11%
Al	13	937 PPM
S	16	811 PPM
Ca	20	637 PPM
Fe	26	109 PPM
Zn	30	24.70 PPM

2. Dosimetric properties

Table 3 shows the calculated surface dose and beam quality at the water phantom for 6, 10, and 15 MV. The surface dose under water, Super-Flex bolus, and CLEANBOLUS were 97.1, 97.4, and 97.1 cGy for the 6 MV photon beam, respectively. Additionally, the beam qualities ($D_{10\,cm}$)

Table 3. Surface dose and beam quality at the water phantom for high-energy MV photon beam

Bolus	Dose (cGy) at water surface					
	6 MV		10 MV		15 MV	
	Surface dose (cGy)	$D_{10\,cm}$ (%)	Surface dose (cGy)	$D_{10\,cm}$ (%)	Surface dose (cGy)	$D_{10\,cm}$ (%)
Water	97.1	66.1	87.5	72.9	83.5	75.9
Super-Flex bolus	97.4	66.0	88.5	72.7	84.2	75.9
CLEANBOLUS	97.1	66.1	87.6	72.8	83.3	75.8

MV, megavoltage.

Table 4. Dosimetric results for Super-Flex bolus and CLEANBOLUS

Thickness	A (nC)	B (nC)	C (nC)
1	3.286	3.286	3.278
2	3.286	3.286	3.278
Average	3.286	3.286	3.278

A, solid water phantom 2 cm; B, solid water phantom 1 cm+Super-Flex bolus 1 cm; C, solid water phantom 1 cm+CLEANBOLUS 1 cm.

Table 5. The volume of unwanted air gap between each bolus and phantom for breast, chin, nose using Super-Flex bolus and CLEANBOLUS

Volume	Super-Flex bolus (cm^3)	CLEANBOLUS (cm^3)
Breast	248.9	108.6
Chin	39.1	6.7
Nose	26.5	21.0

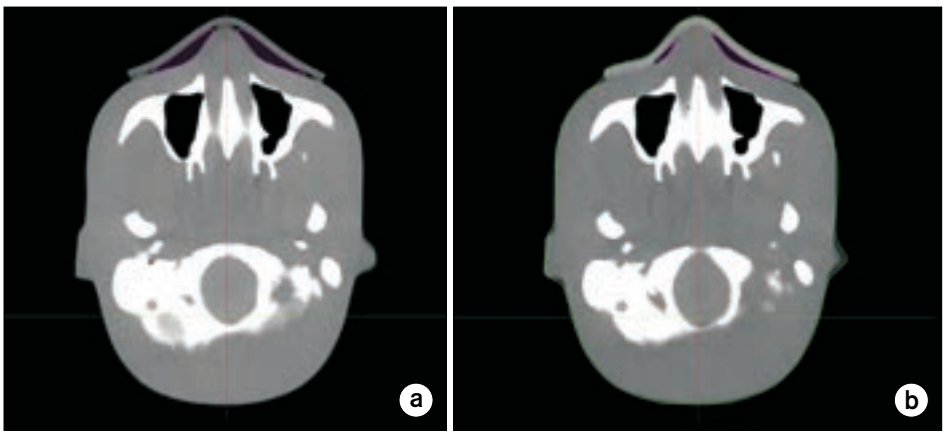

Fig. 2. Unwanted air gap between each bolus and phantom calculated with computed tomography images for nose. (a) Super-Flex bolus. (b) CLEANBOLUS. Pink line means unwanted air gap.

were 66.1%, 66.0%, and 66.1% for water, Super-Flex bolus, and CLEANBOLUS, respectively. Furthermore, the difference in the surface dose and beam quality between the materials under the bolus was not significantly different and independent of the energies. These results indicate that the three materials have similar dosimetric properties. Table 4 shows the measured results for solid water phantom, Super-Flex bolus, and CLEANBOLUS. Also, the measured results of CLEANBOLUS were relatively low, but the ratio was not sufficiently different. Table 5 shows the volume of unwanted air gap for breast, chin, and nose using Super-Flex bolus and CLEANBOLUS. Fig. 2 shows the unwanted air gap between the phantom and each bolus, and the unwanted air gap of CLEANBOLUS was small in the breast, chin, and nose, meaning that it adheres better to the surface.

Discussion

This study evaluated the performance of the newly released CLEANBOLUS, confirming whether it can be used clinically. The HU value of CLEANBOLUS in CT images is 50 on average. Also, the relative electron density to water obtained using the HU-electron density curve is 1.04. This result was obtained from the linear relationship between mass and electron density. However, since this is not always correct, it is necessary to confirm based on dose measure-

ments. Table 4 shows the dosimetric results for CLEANBOUS, meaning that CLEANBOLUS has a similar HU value to solid water phantom within the detector's uncertainty.

The shore hardness of CLEANBOLUS is 000–35, which is good for adherence when placed on an irregular surface. This means that the bolus and skin can be close to minimize unwanted air gap. For high-energy MV photon beams, unwanted air gap reduces the dose delivered to the skin, and several studies have been conducted to reduce unwanted air gap. Anderson et al. [16] investigated a customized bolus using paraffin wax to decrease unwanted air gaps in a standard bolus sheet. Although the customized bolus showed significantly lower complications than a standard sheet bolus, using paraffin wax may result in an irregular thickness. Next, the latest three-dimensional (3D) printers have been used in bolus fabrication. Park et al. [17] developed a method for directly fabricating customized boluses using a 3D printer instead of paraffin wax. They reported that fabrication with a 3D printer could replace unwanted bolus and improve dose distribution. However, because a bolus fabricated using a 3D printer comprises rigid materials, it is challenging to apply to flexible parts. Furthermore, Park et al. [18] recently developed a bolus using mold and casting method with a 3D printer, which successfully overcomes the disadvantages of boluses developed through conventional methods.

However, since it takes a considerable period to manufacture the mold with a 3D printer, it is impossible to use it in a short time. If the bolus is flexible to completely compensate for the curvature of the patient's surface, a 3D-type bolus will not be required. Thus, the low shore hardness of CLEANBOLU has sufficient clinical use potential. In a further study, we will evaluate whether CLEANBOLUS can be applied clinically to minimize unwanted air gap, which was difficult for the existing bolus to solve.

Conclusions

We evaluated the physical and dosimetric properties of CLEANBOLUS because it has characteristics, such as low shore hardness and transparency, and can improve radiation therapy efficiency. As a result, CLEANBOLUS was the most effective and suitable from a clinical perspective. Furthermore, the excellent adhesive strength of CLEANBOLUS reduces unwanted air gaps and ensures an accurate dose distribution.

Acknowledgements

This research was supported by the Basic Science Research Program through the National Research Foundation of Korea (NRF) funded by the Ministry of Education (Grant No. NRF-2019R1F1A1063078).

Conflicts of Interest

The authors have nothing to disclose.

Availability of Data and Materials

All relevant data are within the paper and its Supporting Information files.

Author Contributions

Conceptualization: Jaeman Son. Data curation: Seongmoon Jung. Formal analysis: Jong Min Park. Funding acquisition: Chang Heon Choi. Investigation: Jaeman Son. Methodology: Jung-in Kim. Project administration: Jung-in Kim. Resources: Chang Heon Choi. Software: Jong Min Park. Supervision: Jung-in Kim. Validation: Jaeman Son. Visualization: Seongmoon Jung. Writing–original draft: Jaeman Son and Jung-in Kim. Writing–review & editing: Jaeman Son and Jung-in Kim.

References

1. Fein DA, Mendenhall WM, Parsons JT, Stringer SP, Cassisi NJ, Million RR. Pharyngeal wall carcinoma treated with radiotherapy: impact of treatment technique and fractionation. Int J Radiat Oncol Biol Phys. 1993;26:751-757.
2. Pignon JP, Arriagada R, Ihde DC, Johnson DH, Perry MC, Souhami RL, et al. A meta-analysis of thoracic radiotherapy for small-cell lung cancer. N Engl J Med. 1992;327:1618-1624.
3. Brenner DJ, Hall EJ. Fractionation and protraction for radiotherapy of prostate carcinoma. Int J Radiat Oncol Biol

Phys. 1999;43:1095-1101.
4. Mellenberg DE Jr. Determination of build-up region over-response corrections for a Markus-type chamber. Med Phys. 1990;17:1041-1044.
5. Bilge H, Ozbek N, Okutan M, Cakir A, Acar H. Surface dose and build-up region measurements with wedge filters for 6 and 18 MV photon beams. Jpn J Radiol. 2010;28:110-116.
6. Velkley DE, Manson DJ, Purdy JA, Oliver GD Jr. Build-up region of megavoltage photon radiation sources. Med Phys. 1975;2:14-19.
7. Dogan N, Glasgow GP. Surface and build-up region dosimetry for obliquely incident intensity modulated radiotherapy 6 MV x rays. Med Phys. 2003;30:3091-3096.
8. Ishmael Parsai E, Shvydka D, Pearson D, Gopalakrishnan M, Feldmeier JJ. Surface and build-up region dose analysis for clinical radiotherapy photon beams. Appl Radiat Isot. 2008;66:1438-1442.
9. Price S, Williams M, Butson M, Metcalfe P. Comparison of skin dose between conventional radiotherapy and IMRT. Australas Phys Eng Sci Med. 2006;29:272-277.
10. Weshler Z, Loewinger E, Loewenthal E, Levinson R, Fuks Z. Megavoltage radiotherapy using water bolus in the treatment of Kaposi's sarcoma. Int J Radiat Oncol Biol Phys. 1986;12:2029-2032.
11. Vyas V, Palmer L, Mudge R, Jiang R, Fleck A, Schaly B, et al. On bolus for megavoltage photon and electron radiation therapy. Med Dosim. 2013;38:268-273.
12. Moyer RF, McElroy WR, O'Brien JE, Chamberlain CC. A surface bolus material for high-energy photon and electron therapy. Radiology. 1983;146:531-532.
13. Tieu MT, Graham P, Browne L, Chin YS. The effect of adjuvant postmastectomy radiotherapy bolus technique on local recurrence. Int J Radiat Oncol Biol Phys. 2011;81:e165-e171.
14. Kawamoto T, Shikama N, Kurokawa C, Hara N, Oshima M, Sasai K. Dosimetric assessment of bolus for postmastectomy radiotherapy. Med Dosim. 2021;46:e1-e4.
15. Butson MJ, Cheung T, Yu P, Metcalfe P. Effects on skin dose from unwanted air gaps under bolus in photon beam radiotherapy. Radiat Meas. 2000;32:201-204.
16. Anderson PR, Hanlon AL, Fowble BL, McNeeley SW, Freedman GM. Low complication rates are achievable after postmastectomy breast reconstruction and radiation therapy. Int J Radiat Oncol Biol Phys. 2004;59:1080-1087.
17. Park JM, Lee J, Kim HS, Ye SJ, Kim JI. Development of an applicator for eye lens dosimetry during radiotherapy. Br J Radiol. 2014;87:20140311.
18. Park JM, Son J, An HJ, Kim JH, Wu HG, Kim JI. Bio-compatible patient-specific elastic bolus for clinical implementation. Phys Med Biol. 2019;64:105006.